J|A|C|S
ARTICLES
Published on Web 12/31/2005

Synthesis, Structural, and Electron Topographical Analyses of a Dialkylbiaryl Phosphine/Arene-Ligated Palladium(I) Dimer: Enhanced Reactivity in Suzuki−Miyaura Coupling Reactions

Timothy E. Barder

Contribution from the Department of Chemistry, Massachusetts Institute of Technology, 77 Massachusetts Avenue, Cambridge, Massachusetts 02139

Received September 3, 2005; E-mail: tbarder@mit.edu

Abstract: The treatment of bis(2-(dicyclohexylphosphino)-2′,6′-dimethoxybiphenyl)$PdCl_2$ with $AgBF_4$ produces an air-stable phosphine/arene-ligated Pd(I) dimer with two seemingly identical Pd−arene interactions by X-ray crystallography. However, NMR and theoretical electron topographical analyses of this complex distinguish between these two interactions. One interaction is classified as an arenium-like complex, while the other is classified as a π-interaction. Additionally, this complex is a suitable precatalyst for high yielding Suzuki−Miyaura coupling reactions in short reaction times.

Phosphines as supporting ligands for metals, particularly palladium, have become ubiquitous in the field of cross-coupling chemistry.[1] The continuing examination of structural features of catalyst systems that engender efficacy in coupling processes has become an essential element in ligand design. Particularly, creating not only an electron-rich phosphine center but also modifying other structural features of the phosphine ligand has been valuable in constructing efficient catalysts. In recent years, we have focused on increasing electron density and bulk on the biaryl backbone of 2-dialkylphosphino biaryls (Figure 1).[2] These modifications have created highly reactive and stable catalyst systems for various Pd-catalyzed cross-coupling processes. Recently, we reported the X-ray crystal structure of **1**•Pd(dba)[2b,2d] (where **1** = 2-(dicyclohexylphosphino)-2′,6′-dimethoxybiphenyl and dba = *trans*,*trans*-dibenzylideneacetone) which possesses an η^1-Pd interaction with the 1′ *ipso* carbon. Similar Pd−arene interactions exist with complexes composed of other 2-dicyclohexylphosphino biaryl ligands, such as **2**•Pd(dba) and **3**•Pd(dba),[3] as well as with MOP•Pd(II) and MAP•Pd(II) complexes[4] (where MOP = 2-diphenylphosphino-2′-methoxy-1,1′-binaphthyl and MAP = 2-diphenylphosphino-2′-*N*,*N*′-(dimethylamino)-1,1′-binaphthyl). This unique interaction has been previously suggested to provide stability for the Pd center in both the Pd(II) and Pd(0) states;[2b,4] however, little is known about the physical nature of Pd−arene interactions. In hopes to analyze and further understand these types of interactions, we sought to induce a Pd−arene interaction involving the electron-rich bottom ring of **1** with a highly electrophilic Pd(II) center. Herein, we present our findings and analysis of this endeavor.

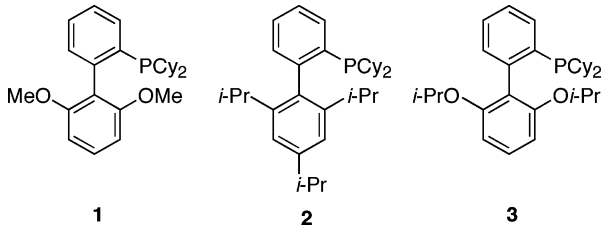

1 **2** **3**

Figure 1. Recently developed 2-dicyclohexylphosphine biaryl ligands.

Synthesis of Complex 6. We recently reported the structure of **4**,[2d] which does not possess any Pd−arene interactions, as the nonphosphine containing ring of the ligand is pointed away from the Pd center. We envisioned treating this complex with a Ag(I) salt to prepare **5** (Figure 2). Complex **5** would possess a highly electrophilic Pd center, which could be stabilized by the nonphosphine containing rings of the ligands. However, when a mixture of **4** and $AgBF_4$ in CH_2Cl_2 was stirred under argon at ambient temperature for 3 h, the desired product, **5**, was not formed, but rather a Pd(I) dimer, **6**, was produced. The deep red complex was isolated from an acetone/ether mixture at −25 °C and crystallized in *C*2/*c* with two tetrafluoroborate counteranions and one acetone molecule. To our surprise, this complex is extremely air-stable in the solid state and solution (dichloromethane); no significant decomposition was observed within 1 week. We attribute this stability to the Pd−arene interactions which shield the Pd centers, thereby preventing them from interacting with oxygen or from self-aggregation.

The synthesis of an analogous dimer was attempted with 2-(2′,4′,6′-tri-*iso*propyl)-dicyclohexylphosphine as the supporting ligand. The reaction appeared to proceed smoothly; however, upon attempted isolation and crystallization, a mixture of Pd

(1) (a) Negishi, E. *Acc. Chem. Res.* **1982**, *15*, 340−348. (b) Negishi, E.; de Meijere, A., Eds. *Handbook of Organopalladium Chemistry for Organic Synthesis*; Wiley-Interscience: New York, 2002. (c) Tsuji, J. *Palladium Reagents and Catalysts*: *New Perspectives for the 21st Century*; John Wiley & Sons Ltd.: Chichester, West Sussex, U.K., 2004.
(2) (a) Huang, X.; Anderson, K. W.; Zim, D.; Jiang, L.; Klapars, A.; Buchwald, S. L. *J. Am. Chem. Soc.* **2003**, *125*, 6653−6655. (b) Walker, S. D.; Barder, T. E.; Martinelli, J. R.; Buchwald, S. L *Angew. Chem., Int. Ed.* **2004**, *43*, 1871−1876. (c) Milne, J. E.; Buchwald, S. L. *J. Am. Chem. Soc.* **2004**, *126*, 13028−13032. (d) Barder, T. E.; Walker, S. D.; Martinelli, J. R.; Buchwald, S. L. *J. Am. Chem. Soc.* **2005**, *127*, 4685−4696.
(3) Barder, T. E.; Buchwald, S. L. Unpublished results.
(4) Kocovsky, P.; Vyskocil, S.; Cisarova, I.; Sejbal, J.; Tislerova, I.; Smrcina, M.; Lloyd-Jones, G. C.; Stephen, S. C.; Butts, C. P.; Murray, M.; Langer, V. *J. Am. Chem. Soc.* **1999**, *121*, 7714−7715.

10.1021/ja0558995 CCC: $33.50

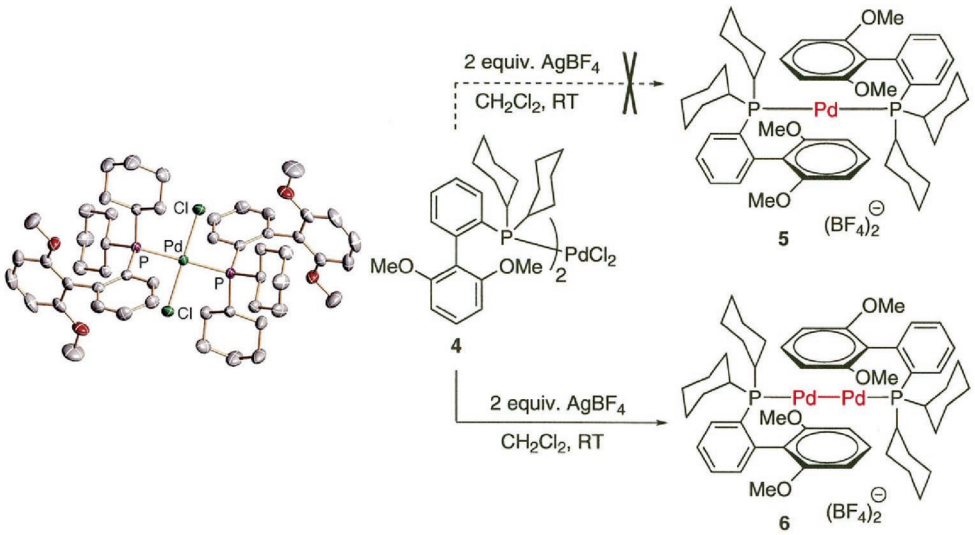

Figure 2. Attempted (dashed arrow) and actual (solid arrow) reactions between $AgBF_4$ and **4** (ORTEP diagram with hydrogens removed for clarity with thermal elliposoids at 30% probability) to produce a dicationic bis-phosphino Pd complex.

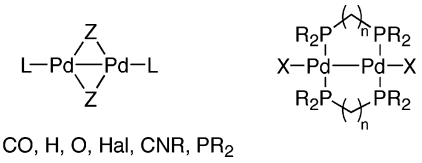

Figure 3. Various types of Pd(I) dimer complexes.

black and free ligand was observed. Additionally, ground-state geometry optimizations were performed on an analogous structure to **6**, but lacking the 2′,6′-dimethoxy groups. A stationary point was found possessing a similar arrangement of the ligands around the Pd centers relative to **6**. However, the electron topographical analyses (namely the bond ellipticity values for the Pd−arene interactions) are drastically different for this structure than for **6**, suggesting both interactions are π-interactions possessing some π-symmetry.[6] These data may suggest that electron-donating groups on the 2′,6′ positions of the ligand are necessary to stabilize the Pd centers.

Background of Pd(I) Dimers. There have been numerous Pd(I) complexes prepared and characterized by X-ray crystallography in the past 60 years;[5] however, the majority of these complexes contain a bridging ligand, which are often CO, hyride, oxygen, halides, isonitriles, and even phosphines (chelating and nonchelating) between the two Pd centers (Figure 3).

Additionally, olefins have been shown to act as bridging ligands between the two Pd centers. However, there have been very few reports of Pd(I) dimer "sandwich" complexes where both Pd centers are positioned between two arenes. One early report of a complex described by Allegra in 1965 and 1970[7] is that of $(Ph•Pd)_2(AlCl_4)_2$ prepared by refluxing $PdCl_2$, Al, and $AlCl_3$ in benzene. An X-ray crystal structure was obtained of this Pd(I) dimer which possessed indistinguishable Pd−$C_{1,1A,6,6A}$ bond distances of 2.34 Å (Figure 4a). More recently, a trinuclear Pd "sandwich" was reported by Sharp (Figure 4b)[8] and a Pd(I) dimer "sandwich" with sulfur based ligands by Pfeffer (Figure 4c).[9] Other interesting Pd(I) dimers possessing Pd−arene interactions include a $(dppp•Pd)_2^{2+}$ complex from van Leeuwen (Figure 4d)[10] and a biarylphosphine Pd(I) dimer complex possessing a bridging bromide from Vilar (Figure 4e)[11] with similar Pd−arene bond lengths to **6**.

Description of the X-ray Crystal Structure of 6. Complex **6** has a Pd−Pd bond length of 2.7037(3) Å, which is consistent with other Pd(I) dimers (Pd−Pd_{min} 2.4878(7), Pd−Pd_{max} 3.1852(6) Å).[12] There exists not only one but two Pd−arene interactions with the nonphosphine containing ring of the biaryl ligand. Curiously, the Pd−C(10A) and Pd−C(7) distances are nearly identical (2.1901(17) and 2.1970(16) Å, respectively), which are substantially shorter than the Pd−P bond length, 2.3045(4) Å (Figure 5). The Pd−C(8) and Pd−C(9A) distances are 2.2989(16) and 2.3870(17) Å, respectively, which are within the sum of the van der Waals radii of Pd and carbon atoms. The C(7)−Pd1 bond length of 2.1970(16) Å is also substantially shorter (by 0.177 Å) than the C(7)−Pd1 bond length in the previously reported structure of **1**•Pd(dba).[2b,d] Unlike the **1**•Pd(dba) X-ray crystal structure where little to no bond length deviations were observed in the nonphosphine containing ring of the ligand relative to **4**, which lacks a Pd−arene interaction, bond length deviations are observed in **6**. The C(7)−C(ortho) distances lengthen from to 1.397(3) and 1.399(3) Å in **4** to 1.453(2) and 1.435(2) Å in **6**, while the O−C(ortho) distances shorten from 1.372(3) and 1.363(3) Å in **4** to 1.345(2) and 1.348(2) Å in **6**.

(5) (a) Murahashi, T.; Kurosawa, H. *Coord. Chem. Rev.* **2002**, *231*, 207−228. (b) Kurosawa, H. *J. Organomet. Chem.* **2004**, *689*, 4511−4520.
(6) The Cartesian coordinates for this optimized structure are included in the Supporting Information. Additionally, the bond ellipticity for the Pd1−C(7) bond critical point is very large (1.042) and for the Pd1−C(10A) bond critical point is much smaller (0.2128). The Pd1−C(7) value clearly illustrates that an elliptical-like orbital (residing both on C7 and C8, but with only one bond critical point to Pd) is interacting with the Pd center, in direct contrast to **6**. For comparison, in the optimized structure of **1**•Pd(dba),[2d] where dba = *trans,trans*-dibenzylidineacetone, there exists an η^2 interaction between Pd and one of the olefins of dba where the Pd−C bond critical points have ellipticity values of 0.7829 and 0.3077.
(7) (a) Allegra, G.; Immirzi, A.; Porri, L. *J. Am. Chem. Soc.* **1965**, *87*, 1394−1395. (b) Allegra, G.; Cassagrande, G. T.; Immirzi, A.; Porri, L.; Vitulli, G. *J. Am. Chem. Soc.* **1970**, *92*, 289−293.
(8) Kannan, S.; James, A. J.; Sharp, P. R. *J. Am. Chem. Soc.* **1998**, *120*, 215−216.
(9) Dupont, J.; Pfeffer, M.; Rotteveel, M. C.; De Cian, A.; Fischer, J. *Organometallics* **1989**, *8*, 1116−1118.
(10) Budzelaar, P. H. M.; Van Leeuwen, P. W. N. M.; Roobeek, C. F.; Orpen, A. G. *Organometallics* **1992**, *11*, 23−25.
(11) Christmann, U.; Vilar, R.; White, A. J. P.; Williams, D. J. *Chem. Commun.* **2004**, 1294−1295.
(12) Murahashi, T.; Otani, T.; Mochizuki, E.; Kai, Y.; Kurosawa, H. *J. Am. Chem. Soc.* **1998**, *120*, 4536−4537.

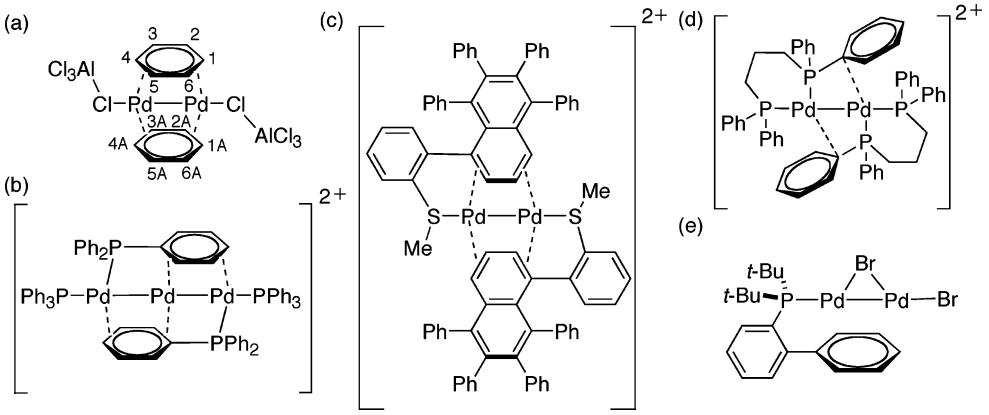

Figure 4. Isolated and Characterized Pd(I) complexes.

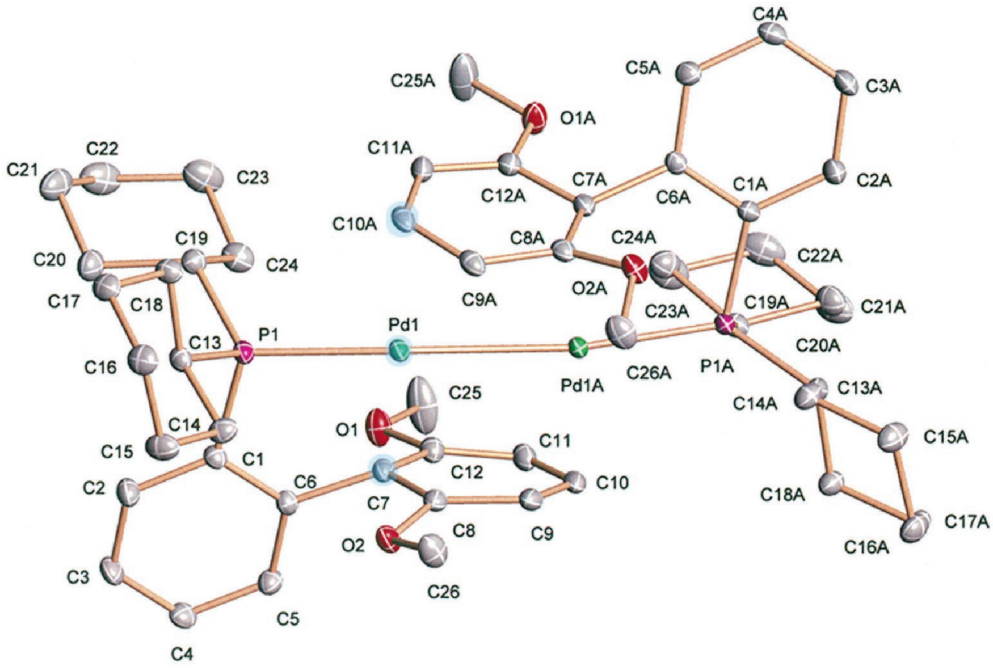

Figure 5. ORTEP diagram of **6** with hydrogens, acetone, and tetrafluoroborate anions removed for clarity. Thermal ellipsoids at 50% probability.

Selected Bond Lengths (Å) and Angles (deg)

Pd(1)−Pd(1A) 2.7037(3)	Pd(1)−P(1) 2.3045(4)
Pd(1)−C(8) 2.2989(16)	Pd(1)−C(10A) 2.1901(17)
Pd(1)−C(7) 2.1970(16)	Pd(1)−C(9A) 2.3870(17)
C(7)−C(12) 1.453(2)	O(1)−C(12) 1.348(2)
C(7)−C(8) 1.435(2)	O(2)−C(8) 1.345(2)
P(1)−Pd(1)−Pd(1A) 169.596(12)	C(7)−Pd(1)−C(10A) 170.26(7)
C(6)−C(7)−Pd(1) 114.32(11)	C(10)−C(7)−Pd(1) 88.41

These bond length deviations suggest an arenium ion[13] (also commonly referred to as a σ complex or Wheland intermediate) has formed, where the bottom ring of the ligand has undergone electrophilic addition to the Pd center and is stabilized by an *ortho* methoxy group. The 172 ppm (broad singlet) ^{13}C NMR chemical shift of C8 suggests substantial double bond character in the O(2)−C(8) bond, which is consistent with the formation of a stabilized arenium ion.[4] Further evidence from electron topography analyses for this complex existing as a stabilized arenium ion is provided below.

Suzuki−Miyaura Reactions Utilizing 6. As **6** is composed of a 1:1 ratio of ligand:Pd, which is believed to be the ratio of the active catalyst in cross-coupling reactions with 2-phosphinobiaryl based ligands,[2d,14] Suzuki−Miyaura coupling reactions were attempted with **6** as the precatalyst. Heating the reaction mixture composed of an aryl boronic acid, aryl chloride, base, and **6** to temperatures ≥ 90 °C caused rapid formation of Pd black, which is most likely due to the lack of excess ligand to stabilize the Pd after reduction to the zero oxidation state. However, decreasing the reaction temperature to 70 °C in toluene prevented the formation of Pd black, and reactions of even trisubstituted biaryls proceeded smoothly and very rapidly (Table 1, entry 1). This is further evidence that the catalytic cycle is composed of a monoligated-Pd rather than a bis-ligated-Pd center as with other smaller ligands, i.e., triphenylphosphine or even tri-*tert*-butylphosphine. Additionally, arenes possessing sensitive functional groups, such as 3-chlorobenzaldehyde, reacted quickly with 2-methoxyphenylboronic acid in 92% isolated yield using only 0.2% **6** in 1 h at 70 °C (Table 1, entry

(13) Olah, G. A. *J. Am. Chem. Soc.* **1971**, *94*, 808−820.

(14) Strieter, E. R.; Blackmond, D. G.; Buchwald, S. L. *J. Am. Chem. Soc.* **2003**, *125*, 13978−13980 and references therein.

Scheme 1. Proposed Reduction of **6** to **1**•Pd(0) by Phenylboronic Acid

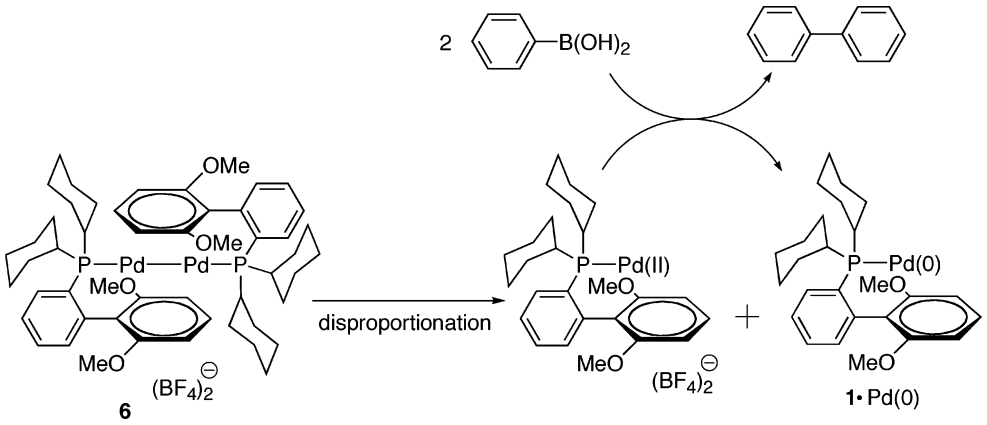

Table 1. Suzuki−Miyaura Couplings Using **3** as the Precatalyst[a]

Entry	Aryl Chloride	Aryl Boronic Acid	Product	Time/h	%Yield
1	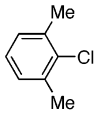	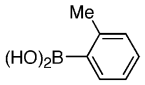	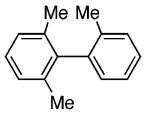	1	96
2		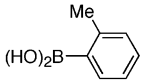	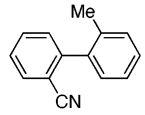	0.5	99
3	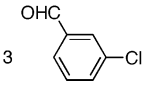	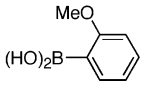	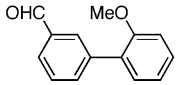	1	92

[a] Reaction conditions: 1 mmol of ArCl, 1.5 mmol of $ArB(OH)_2$, 2 mmol of K_3PO_4, 0.2 mol % **3**, 0.5 M PhMe, 70 °C.

3). Bis(phosphine)-μ-bromide Pd(I) dimers have also been used in the amination of aryl halides, Suzuki−Miyaura coupling reactions, and α-arylation of ester enolates.[10,15]

In all examples in Table 1, the reaction mixture containing the red complex, **6**, immediately changed color to yellow or beige upon heating. This color change is likely due to the rapid reduction of **6** to **1**•Pd(0) by the aryl boronic acid with concurrent generation of the respective biaryl (Scheme 1). Most likely, disproportionation occurs to form a monoligated-Pd(0) and a monoligated-Pd(II) species. Reduction of the Pd(II) species can then occur by the aryl boronic acid. To initially probe the activation of **6**, the reaction of *o*-tolyl boronic acid and 2-chloro-*m*-xylene with 0.2% **6** was conducted at 40 °C for 1 h. This reaction is identical to the reaction in Table 1, entry 1 (for which a 96% yield was obtained) except for the lower temperature. However, only ∼25% conversion of the aryl chloride was observed when the reaction temperature was 40 °C. Surprisingly, the much easier reaction of *o*-tolyl boronic acid with 4-*n*-butylchlorobenzene only proceeded to ∼50% conversion of aryl chloride using 0.2% **6** in 1 h at 40 °C. Since disproportionation of **6** yields both a monoligated Pd(II) and Pd(0) species (the presumed active catalyst), the reaction of *o*-tolyl boronic acid with 4-*n*-butylchlorobenzene should proceed very rapidly if disproportionation readily occurs at 40 °C as there would be ∼0.1% of the highly reactive monoligated-Pd(0) species present even if the reduction of the monoligated-Pd(II) species was difficult at this temperature. These results initially suggest that higher temperatures are required for the disproportionation of **6**. However, as the reduction of biaryl phosphine Pd(II) species (a key step in the mechanism proposed in Scheme 1) is not yet understood, further studies on the activation of **6** will be conducted after more data are amassed regarding the reduction of biaryl phosphine Pd(II) complexes.

Atoms in Molecules and ELF Analyses. To further explore the electronic nature of this complex, we turned to electron topography techniques. Although specialized high resolution X-ray diffraction techniques exist that locate bonding electrons, standard X-ray diffraction techniques only locate electron density surrounding but not between atoms (i.e., bonds). The theory of *Atoms in Molecules* developed by Bader[16] allows for the topographical analysis of electron density, $\rho(r)$, and location and analysis of extrema, i.e., critical points, within the electron density. In particular, the existence of a bond path containing a bond critical point (3, −1), where 3 is the rank, ω, i.e., number of nonzero eigenvalues (curvatures) in standard Cartesian coordinates, and −1 is the signature, σ, i.e., the sum of the signs of the three nonzero eigenvalues (curvatures), confirms the presence of a bonding interaction. However, the rank and signature do not allow for further analyses of the nature of the bond, and more in depth topographical values were required. Additionally, the electron localization function (ELF) of Becke and Edgecombe[17] which was further developed by Silvi and Savin[18] provides insight into the classification of chemical bonds by visualization of valence shell regions in molecules.

All calculations were conducted on a home-built Linux cluster consisting of 24 Xeon processors. The ground-state optimization of $(\mathbf{1})_2Pd_2^{2+}$ was completed using Gaussian 03[19] with the B3LYP hybrid functional.[20] For C, H, O, and P atoms, the 6-31G(d) basis set was used, and for the Pd center, LANL2DZ+ ECP[21] was employed. The X-ray structure coordinates were used as a starting point for the optimization which was constrained to *C*2 symmetry. Due to the large size of this calculation, a

(15) (a) Hooper, M. W.; Utsunomiya, M.; Hartwig, J. F. *J. Org. Chem.* **2003**, *68*, 2861−2873. (b) Jørgensen, M.; Lee, S.; Liu, X.-X.; Wolkowski, J. P.; Hartwig, J. F. *J. Am. Chem. Soc.* **2002**, *124*, 12557−12565. (c) Stambuli, J. P.; Kuwano, R.; Hartwig, J. F. *Angew. Chem., Int. Ed.* **2002**, *41*, 4746−4748.

(16) Bader, R. F. W. *Atoms in Molecules*; Oxford Unversity Press: New York, 2003.
(17) Becke, A. D.; Edgecombe, K. E. *J. Chem. Phys.* **1990**, *92*, 5397−5403.
(18) Silvi, B.; Savin, A. *Nature* **1994**, *371*, 683−686.
(19) Frisch, M. J., et al. *Gaussian 03*, revision B.05; Gaussian, Inc.: Pittsburgh, PA, 2003.
(20) (a) Becke, A. D. *J. Chem. Phys.* **1993**, *98*, 5648−5652. (b) Lee, C.; Yang, W.; Parr, R. G. *Phys. Rev. B* **1988**, *37*, 785.
(21) Hay, P. J.; Wadt, W. R. *J. Chem. Phys.* **1985**, *82*, 299−310.

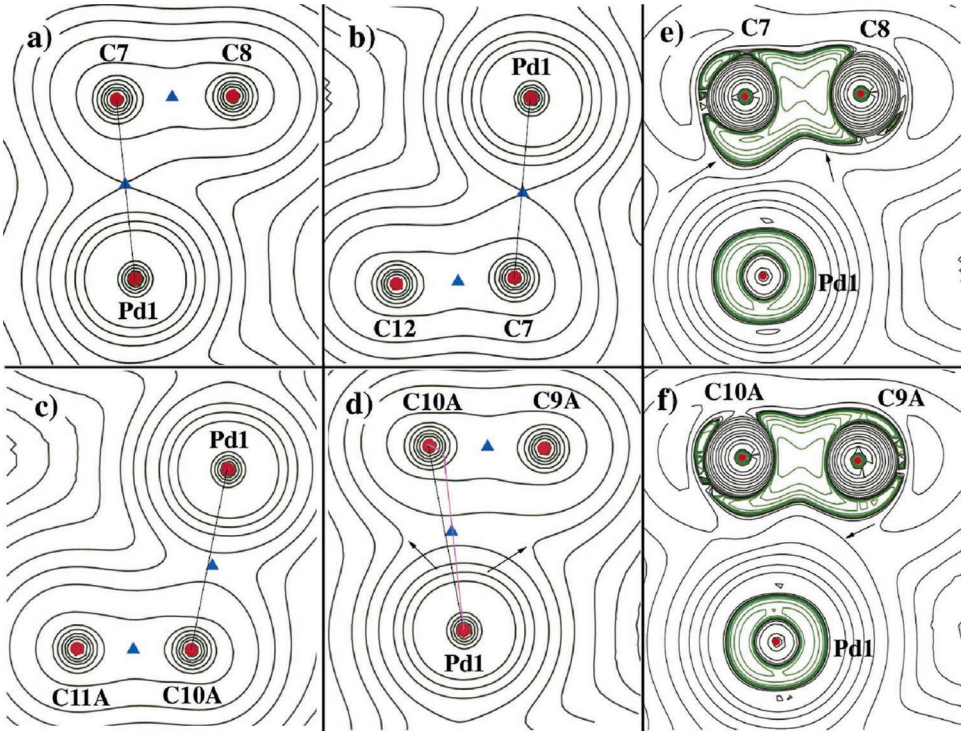

Figure 6. Contour diagrams of $\rho(r)$ [a, b, c, d] and $\nabla^2\rho(r)$ [e, f] (black contours = positive values, green contours = negative values) for various planes in **6**. The red circles are (3, −3) critical points, the blue triangles are (3, −1) critical points, and the pink curve in [d] is the bond path connecting Pd1−C(10A). Contour values for [a−d]: 0.001, 0.002, 0.004, 0.008, 0.02, 0.04, 0.08, 0.2, 0.4, 0.8. Those for [e, f]: −40, −20, −10...10, 20, 40.

frequency calculation to ensure all positive eigenvalues could not be conducted; however, $(\mathbf{1})_2Pd_2^{2+}$ was optimized to convergence criteria as follows: RMS force = 0.000 003 hartrees/bohr and RMS atom displacement = 0.000 343 hartrees/radian, with $\partial E/\partial X_n = 0.0$ (n = 980). Subsequently, a single-point energy calculation with concurrent generation of a wave function file was conducted at 6-311++G(2d,2p) for C, H, O, and P and LANL2DZ+ECP[21] for Pd. The wave function file was analyzed by AIM2000.[22] For the ELF analysis, a formatted checkpoint file was used employing the program DGrid 3.0.[23] The files generated by these programs were visualized using VMD[24] and MOLEKEL.[25]

It is important to note that the optimized structure of **6** is not identical to that of the X-ray crystal structure.[26] However, the structure is very similar with key bond distance differences of Pd1−C(7) 0.06 Å, Pd1−C(10A) 0.11 Å, and Pd1−Pd1A 0.15 Å. In the optimized structure, from which further discussion is based, the bond length difference between the Pd1−C(7) and Pd1−C(10A) is only 0.06 Å.

Contour diagrams of $\rho(r)$ and $\nabla^2\rho(r)$ of four different planes containing the Pd center and carbon atoms nearest the metal center are depicted in Figure 6. The red circles represent (3, −3) critical points which are local maxima in $\rho(r)$, i.e., nuclei, while the blue triangles represent (3, −1) critical points which are saddle points in $\rho(r)$. In Figure 6a−d there exists only one

Table 2. Selected Topographical Values for **6**[a]

A_i–A_j	r_i	r_j	$\rho(r_c)$	$\nabla^2\rho(r_c)$	λ_1	λ_2	λ_3	ϵ
Pd−C(7)	2.289	1.972	0.0740	0.1592	−0.0757	−0.0718	0.3066	0.0540
Pd−C(10A)	2.358	2.014	0.0618	0.1502	−0.0614	−0.0522	0.2637	0.1754
C(7)−C(8)	1.410	1.348	0.2620	−0.5186	−0.4965	−0.4158	0.3938	0.1942
O−C(8)	1.673	0.907	0.2643	−0.3381	−0.4701	−0.4640	0.5961	0.0132

[a] All values in atomic units.

(3, −1) critical point between Pd1−C(n), n = 7, 10A. However, in Figure 6d, the contours to which the arrows point widen relative to those in Figure 6a−c. This is suggestive of the presence of an interaction between Pd1−C(9A), although neither a (3, −1) nor a (3, +1) critical point (i.e., a ring critical point (3, +1) which would be present within the triangle formed by Pd1−C(10A)−C(9A)) could not be located despite numerous attempts. Additionally, the (3, −1) critical point between Pd1−C(10A) in Figure 6c and 6d does not lay directly on the Pd1−C(10A) bond, as it does in Figure 6a and 6b, but is slightly shifted to the right, i.e, toward C(9A); the pink line in Figure 6d depicts the actual bond path between Pd1−C(10A). This slight shift is noteworthy as is described in the following section. There are two striking differences in the plots of $\nabla^2\rho(r)$ for the Pd1−C(7)−C(8) plane compared to the Pd1−C(10A)−C(9A) plane. The area of charge concentration between C(7) and Pd1 (Figure 6e, leftmost arrow) is much greater than that compared to Figure 6f. Additionally, the contour to which the rightmost arrows point in Figure 6e and 6f encompasses the C(7) and C(8) atoms, while the corresponding contour in Figure 6f surrounds the Pd center. This is likely due to the (3, −1) critical point between Pd1−C(10A) slightly shifting toward C(9A), such that the bond is becoming more centered between C(10A) and C(9A) relative to the Pd1−C(7) bond.

(22) Biegler-König, F.; Schönbohm, J.; Bayles, D. *J. Comput. Chem.* **2001**, *22*, 545−559.
(23) Kohout, M. *DGRID*, edition 3.0; Max Planck Institute of Chemical Physics of Solids: Dresden, 2005.
(24) Humphrey, W.; Dalke, A.; Schulten, K. VMD - Visual Molecular Dynamics. *J. Mol. Graphics* **1996**, *14*, 33−38.
(25) Flükiger, P.; Lüthi, H. P.; Portmann, S.; Weber, J. *MOLEKEL 4.0*; Swiss Center for Scientific Computing: Manno, Switzerland, 2000.
(26) See the Supporting Information for the Cartesian coordinates for the optimized structure of $(\mathbf{1}\bullet Pd)_2^{2+}$.

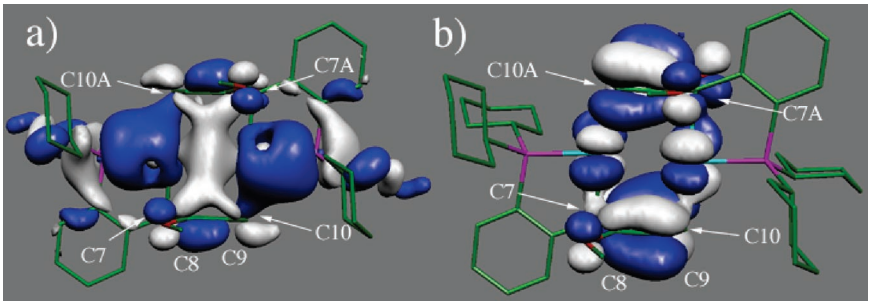

Figure 7. Molecular orbital diagrams of **6**, green = carbon, red = oxygen, pink = phosphorus. The Pd centers are located within the surface of the MOs. (a) HOMO (−0.392 eV), (b) HOMO-1 (−0.399 eV).

Selected electron topographical values for **6** are presented in Table 2. The most striking values for **6** are the vastly different bond ellipticity values, ϵ, defined as $(\lambda_1/\lambda_2 - 1)$. The bond ellipticity is the ratio of the smallest eigenvalue to the other negative eigenvalue (only two negative eigenvalues exist for a bond critical point). By comparing λ_1 and λ_2, i.e., the amount of depletion of electron density from the saddle point, in the direction of the two negative eigenvalues, the bond symmetry can be analyzed. If $\lambda_1 = \lambda_2$, then $\epsilon = 0$, which is the case for a pure sigma bond. For a pure sigma bond, the depletion of electron density from the bond critical point in the direction of the two negative eigenvalues is equal, which creates a cylindrical shape of electron density. However, if $|\lambda_1| > |\lambda_2|$, then $\epsilon > 0$ is obtained. In this case, the bond possesses varying amounts of π character; the greater the absolute value of the ratio of λ_1 to λ_2, the greater the amount of π character. Hence, the cylindrical shape of electron density, observed when $\epsilon = 0$, stretches to an ellipse. As a standard reference, in ethane, benzene, and ethylene, the C−C bond critical points have values of $\epsilon = 0.0, 0.2, 0.33$.[27]

The values of ϵ for the (3, −1) critical point of Pd1−C(7) and Pd1−C(10A) of the ground-state optimized structure of **6** provide insight into the symmetry of the bond that is present. Namely, for the Pd1−C(7) bond, $\epsilon = 0.0540$, while for the Pd1−C(10A) bond, a value nearly 4 times greater is observed, $\epsilon = 0.1754$. This difference is substantial as both the Pd−C(7) and Pd1−C(10A) bonds are identical in length in the X-ray crystal structure and very similar in the optimized structure (Pd1−C(7) 2.25 Å, Pd−C(10A) 2.31 Å). Additionally, the value of $\rho(r_c)$ for the Pd1−C(7) bond critical point is slightly greater (0.0128), suggesting a stronger bond than Pd1−C(10A). The large difference in bond ellipticity, difference in $\rho(r_c)$ for the (3,−1) critical points of Pd1−C(7) and Pd1−C(10A), and shift of the (3,−1) bond critical point toward C(9A) are strong indications that the Pd1−C(10A) bond is composed of some π character while the Pd1−C(7) bond is composed of mostly σ character. This concept is consistent with the ^{13}C NMR spectrum obtained of **6**, as described above. The upper half of the aromatic ring (C7−C8−C12) of the ligand exists as an arenium ion (hence the mainly σ character in the Pd−C(7) bond) with the Pd center stabilized by an *ortho* methoxy group. However, the lower half of the aromatic ring (C9−C10−C11) of the ligand interacts with the Pd centers through both a cylindrical C10(p_z) (the arrow pointing to the blue surface from C10 in Figure 7a) orbital and an elliptical-like orbital (the arrow pointing to the white surface from C10 in Figure 7b) residing on C10 and C9.

(27) Koritsanszky, T.; Buschmann, J.; Luger, P. *J. Phys. Chem.* **1996**, *100*, 10547−10553.

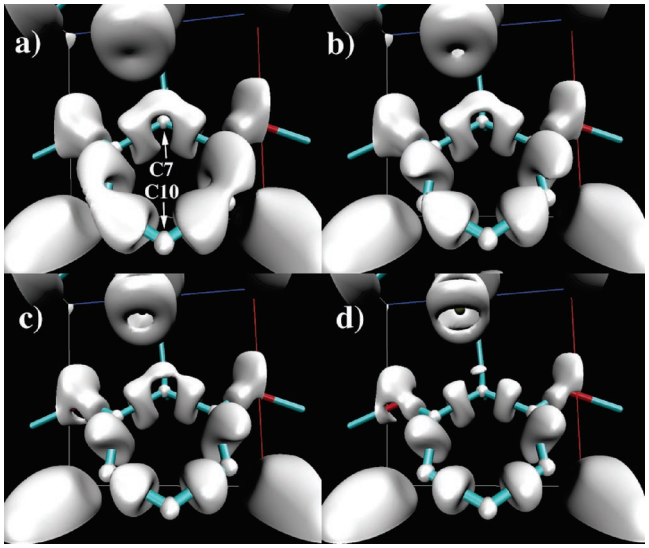

Figure 8. Electron localization function (ELF) plots of the nonphosphine containing ring of the ligand in **6**, torquoise = carbon−carbon bonds and red = oxygen−carbon bonds. ELF isosurface value (a) 0.67, (b) 0.70, (c) 0.74, (d) 0.78.

The contributions from both the HOMO and HOMO-1, which are very similar in energy (0.007 eV difference), may produce an elliptical-like orbital, residing mainly on C10 and slightly on C9. This orbital may interact with the Pd center, causing the value of ϵ at the (3, −1) critical point between Pd1−C(10A) to be nearly 4 times greater than that at the (3, −1) critical point between Pd1−C(7). Additionally, the presence of this elliptical-like orbital helps explains the shifting of the (3, −1) critical point toward C(9A) thereby creating a bond possessing some π symmetry.

Finally, we plotted the electron localization function (ELF) to assist in visualizing the valence shell regions of the nonphosphine containing ring of the ligand in **6** (Figure 8). Figure 8a−d clearly depict ELF isosurfaces encapsulating C(7), while no such encapsulation exists around C(10). The lack of encapsulation around C(10) is likely due to the C10(p_z) orbital being utilized in the Pd1−C(10A) interaction, i.e., the valence shell electrons are occupied in the Pd1−C(10A) interaction. However, as the Pd1−(C7) bond is mainly a σ interaction, the valence shell electrons of C(7) are accessible and are able to be visualized.

In conclusion, we have synthesized and characterized a novel phosphine/arene ligated Pd(I) dimer in the solid and solution state. This dimer is a suitable precatalyst for efficient and rapid Suzuki−Miyaura cross-coupling reactions. Additionally, electron topography studies were conducted that shed light on the true

nature of the seemingly identical two arene−Pd interactions. The solid and solution state experimental data agree well with the theoretical data: although two bonds may be nearly identical in bond length and type of atoms involved, the electronic properties of the bond are ever so important in determining the nature of the bond. Namely, we classify the Pd−arene interaction with proximal methoxy groups as an arenium ion (σ complex), while the Pd−arene interaction distal from the methoxy groups is mainly a π interaction possessing some π symmetry due the indirect bond path linking Pd1−C(10A). Further analyses to determine the importance of Pd−arene interactions of dialkylbiaryl phosphine ligated Pd complexes that lay within the catalytic cycles of amination and Suzuki−Miyaura coupling reactions are in progress.

Acknowledgment. We thank the National Institutes of Health (GM 46059) for support for this work. We are grateful to Merck for additional support. We thank Engelhard for supplying the $PdCl_2$ used in this work. T.E.B. is grateful to Professor Steve Buchwald for the freedom that made this work possible as well as his support and encouragement. T.E.B. also thanks Professor Kit Cummins for providing insightful advice, Professor Ged Parkin for stimulating discussions, and Drs. Bill Davis and Peter Müller for assistance with the solvent disorders in the X-ray crystal structures. Additionally, T.E.B. thanks one of the reviewers for suggesting important and insightful experiments regarding the activation of **6**.

Supporting Information Available: Experimental procedures, spectral data, coordinates for the calculated structures, X-ray crystal structure data (PDF), and the complete list of authors for ref 18. This material is available free of charge via the Internet at http://pubs.acs.org.

JA0558995